Ab initio optimized pseudopotential calculations of magnetic systems

Taizo Sasaki,* Andrew M. Rappe,† and Steven G. Louie
Department of Physics, University of California at Berkeley, Berkeley, California 94720
and Materials Sciences Division, Lawrence Berkeley Laboratory, Berkeley, California 94720
(Received 17 May 1995; revised manuscript received 11 July 1995)

The structural and magnetic properties of ferromagnetic iron and nickel are computed using a plane-wave basis set and the optimized pseudopotentials to study the effectiveness of these methods for magnetic systems within the local-spin-density approximation. Although the pseudo wave functions deviate significantly from the all-electron wave functions in the core region, the calculated structural and magnetic properties are in excellent agreement with results obtained from all-electron calculations. The present results thus show that it is possible to apply the optimized pseudopotentials to magnetic systems using the convenient formalism of plane-wave basis sets.

I. INTRODUCTION

Recent progress in pseudopotential theory[1–3] has reduced the size of the plane-wave basis set required to perform local-density-functional calculations for a wide variety of materials, including first-row and 3*d* elements. The optimized pseudopotential proposed by Rappe *et al.*[1] has been applied to solid copper, and an accurate description of its structural properties was obtained with a small number of plane-wave functions. Similar efficiency has been achieved by Troullier and Martins,[2] Vanderbilt,[3] and others using a variety of other pseudopotential generation schemes. However, application of these pseudopotentials has so far been limited to nonmagnetic materials. In this work, we investigate the effectiveness of the optimized pseudopotentials generated using the method of Ref. 1 for the calculation of the properties of magnetic materials within the local-spin-density approximation (LSDA).

The pseudopotential approximation is motivated by the fact that the behavior of the valence electrons in the bonding region primarily determines the electronic structure and the structural properties of many materials. In a pseudopotential formulation, the effect of the core electrons and that of the nuclear potential are combined to form an effective ionic pseudopotential. The pseudopotentials are commonly constructed, so that outside of a core region the valence pseudo wave functions match the corresponding states derived from an all-electron calculation, and inside this region they are smooth functions. This formulation makes pseudopotential calculations quite efficient, since the core orbitals do not need to be recomputed. In addition, because the behavior of the pseudo wave functions inside the core region need not match that of the all-electron wave functions (see Fig. 1), the number of plane waves required to describe them may be drastically reduced.

In contrast to the properties mentioned above, the magnetic properties of transition metals originate from the *d* electrons which have large wave-function amplitudes near the core region. Accordingly, it would appear that it is important to describe the behavior of the wave functions in the core region as accurately as possible to obtain precise results. In previous investigations[4,5] on magnetic materials with the pseudopotential method, the pseudo wave function for the localized state, in fact, deviates only slightly from the all-electron wave function due to a small core radius employed. Thus, it is not clear whether the optimized pseudopotential which gives rise to a pseudo wave function that deviates significantly from the all-electron wave function in the core region can be applied successfully to magnetic materials.

Conventionally, the study of magnetic materials has been performed using all-electron LSDA electronic-structure calculations employing the linear augmented plane-wave (LAPW), Korringa-Kohn-Rostoker (KKR), and linear muffin-tin orbital (LMTO) methods. However, the basis sets used in these methods have their limitations. In general, they are complicated numerical functions, which makes them difficult to use for the calculation of forces, response functions, and many-body effects going beyond the LSDA. For example, unlike plane waves, such basis functions depend on atomic positions, and therefore additional calculation of the Pulay force terms is required to obtain atomic forces. Basis sets, such as those used in Refs. 4 and 5, which mix localized orbitals with plane waves encounter similar problems. If optimized pseudopotentials can provide accurate results for magnetic materials, the simplicity of the plane-wave basis set would make applications beyond total-energy calculations much easier for these materials.

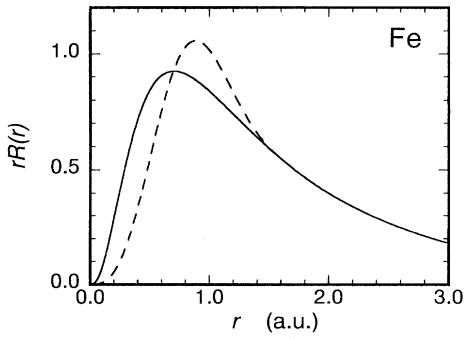

FIG. 1. 3*d* radial wave functions of iron. The solid and broken lines are the all-electron wave function and the pseudo wave function, respectively.

TABLE I. Comparison of the 3*d* eigenvalues and the excitation energies at different configurations. Super- and subscripts of each configuration denote the number of majority and minority spins, respectively. Values in parentheses are the deviations from the all-electron results. (AE = all-electron, PS = pseudopotential, and all energies are in Ry.)

Element	configuration		Majority spin	Minority spin	Exchange splitting	Excitation energy
Fe^0	$(3d)^5_1(4s)^1_1$	AE	-0.683	-0.433	0.250	
		PS	-0.689 (-0.006)	-0.424 (0.009)	0.265 (0.015)	
	$(3d)^4_2(4s)^1_1$	AE	-0.645	-0.520	0.126	0.188
		PS	-0.648 (-0.003)	-0.516 (0.004)	0.132 (0.006)	0.199 (0.011)
	$(3d)^5_1(4s)^1_0(4p)^1_0$	AE	-0.784	-0.507	0.277	0.211
		PS	-0.790 (-0.006)	-0.497 (0.010)	0.292 (0.015)	0.211 (0.000)
Fe^{2+}	$(3d)^5_1(4s)^0_0$	AE	-2.023	-1.758	0.266	1.832
		PS	-2.031 (-0.008)	-1.750 (0.008)	0.281 (0.015)	1.833 (0.001)
	$(3d)^4_1(4s)^1_0$	AE	-2.480	-2.241	0.239	2.468
		PS	-2.503 (-0.023)	-2.252 (0.011)	0.251 (0.012)	2.484 (0.016)
Ni^0	$(3d)^5_3(4s)^1_1$	AE	-0.758	-0.623	0.135	
		PS	-0.760 (-0.002)	-0.621 (0.002)	0.139 (0.004)	
	$(3d)^4_4(4s)^1_1$	AE	-0.697	-0.697	0	0.068
		PS	-0.697 (0.000)	-0.697 (0.000)	0 (0)	0.069 (0.001)
	$(3d)^5_3(4s)^1_0(4p)^1_0$	AE	-0.878	-0.724	0.154	0.269
		PS	-0.881 (-0.003)	-0.722 (0.002)	0.158 (0.004)	0.269 (0.000)
Ni^{2+}	$(3d)^5_3(4s)^0_0$	AE	-2.186	-2.047	0.139	1.967
		PS	-2.191 (-0.005)	-2.048 (-0.001)	0.143 (0.004)	1.968 (0.001)
	$(3d)^4_3(4s)^1_0$	AE	-2.664	-2.570	0.094	2.684
		PS	-2.688 (-0.024)	-2.592 (-0.022)	0.096 (0.002)	2.698 (0.014)

To investigate the effectiveness of the optimized pseudopotentials for magnetic systems, we have applied them to isolated atoms and bulk solids of the prototypical transition metals, iron and nickel. To compare the result with previous works, the calculations are performed within the LSDA (Ref. 6) of density-functional theory,[7] even though the LSDA is known to give an incorrect ground state for iron.[8,5] The exchange-correlation potential used is that of Ceperley and Alder[9] as parametrized by Perdew and Zunger.[10] Since we are considering the 3*d* elements, relativistic effects are neglected.

In the remaining part of this paper, optimized pseudopotentials are presented and applied to isolated atoms with spin-polarized configurations in order to explore their validity (Sec. II). These pseudopotentials are then applied to bulk Fe and Ni (Sec. III). The results of our electronic-structure calculations are then compared to those previously obtained with all-electron methods. Section IV summarizes the present study.

II. THE OPTIMIZED PSEUDOPOTENTIAL AND ITS APPLICATION TO ATOMS

The optimized norm-conserving pseudopotential[1] is generated by minimizing the quantity defined by

$$I(q_c)=\int d\mathbf{r}\psi^*(\mathbf{r})(-\nabla^2)\psi(\mathbf{r})-\int_{q<q_c}\frac{d\mathbf{q}}{(2\pi)^3}q^2|\psi(\mathbf{q})|^2. \tag{2.1}$$

The first term in this expression is the kinetic energy of the pseudo wave function $\psi(\mathbf{r})$, while the second term is the portion of the kinetic energy of $\psi(\mathbf{r})$ which is contained in plane waves with wave vectors less than q_c. Therefore, the expression $I(q_c)$ represents the kinetic energy convergence error, the amount of kinetic energy neglected by expressing $\psi(\mathbf{r})$ in a truncated basis set of plane waves. Since it can be shown[1] that the convergence of the total energy and that of the kinetic energy behave similarly, $I(q_c)$ provides an excellent estimate of the error in the computed total energy of solids due to using a plane-wave cutoff at q_c.

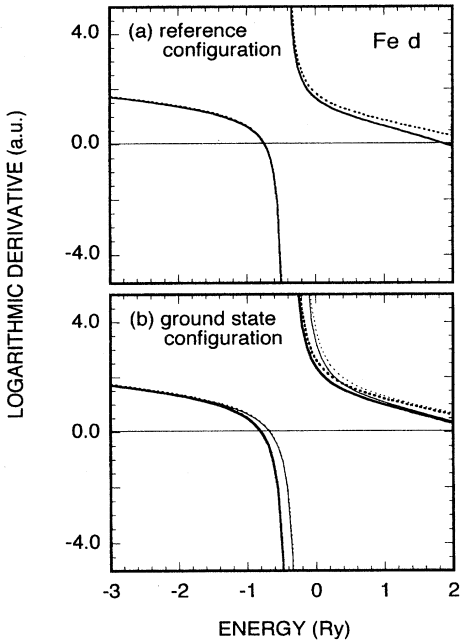

FIG. 2. Logarithmic derivatives of d wave functions of iron at $r=2.2$ a.u. (a) for the reference configuration and (b) for the ground-state configuration. The solid lines are for all-electron wave function and the broken lines are for pseudo wave function. In the panel (b), thick lines and thin lines are for the majority- and minority-spin states, respectively.

The optimized pseudopotential method seeks to make the convergence error as small as possible by minimizing $I(q_c)$ subject to the constraints that $\psi(\mathbf{r})$ match the all-electron wave function outside a real-space cutoff radius r_c with smoothness up to the second derivative of $\psi(\mathbf{r})$ at $r=r_c$, and that $\psi(\mathbf{r})$ obeys the norm conservation condition.[11] Although the exact minimization can generate a pseudopotential with a cusp at r_c, it can be effectively avoided by using a finite set of basis functions to describe the atomic pseudo wave functions. The parameter q_c in Eq. (2.1) determines the convergence of the kinetic energy with respect to the plane-wave cutoff energy in k-space calculations. In practical calculations, q_c is increased until the convergence error $I(q_c)$ is acceptable.

In order to obtain a soft and accurate pseudopotential, we set r_c of the $3d$ orbitals at 1.6 a.u. which is about twice the distance from the nucleus to the peak position of the all-electron wave function. This choice of r_c makes $I(q_c)$ less than 1 mRy at $q_c = 8$ and 8.7 a.u. for iron and nickel, respectively. The reference configuration in the generation of the pseudopotential is taken to be $(3d)^n(4s)^{1.75}(4p)^{0.25}$ without spin polarization, where n is the number of d electrons in the neutral atom. The $3d$ pseudo wave function of iron is depicted in Fig. 1. As a result of the large r_c, significant deviation from the all-electron wave function can be seen.

The $3d$ eigenvalues and the excitation energies for the various spin-polarized configurations are listed in Table I. Since there is a significant overlap between valence and core charge densities, the latter is explicitly retained in the calculation of the exchange-correlation energies and potentials using the scheme of Louie *et al.*[12] From this table, we see that the one-electron eigenvalues and the excitation energies are reproduced quite accurately with the pseudopotential in the various spin-polarized configurations. The maximum error in the magnitude of the exchange splitting, the difference between eigenvalues of majority and minority spins, is 6% of the all-electron result. The deviations of the $4s$ and $4p$ eigenvalues are less than 1%.

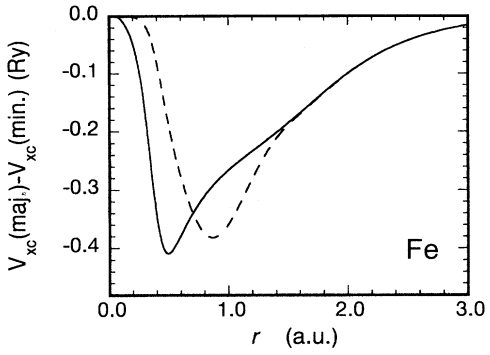

FIG. 3. The difference in the exchange-correlation potentials for the majority- and minority-spin states of iron. The solid line is for the all-electron result and the broken line is for the pseudopotential result. The configuration is taken to be $(3d)^5_1(4s)^1_1$.

As a further examination on the total-energy-related quantities, we study the intra-atomic Coulomb correlation ener-

TABLE II. Comparison of the theoretical structural parameters of bcc iron and fcc nickel. E_{pw} is the plane-wave cutoff energy.

	Method	Lattice constant (a.u.)	Bulk modulus (Mbar)	Cohesive energy (eV)
Fe	Present work			
	E_{pw} = 60 Ry	5.26	2.71	6.32
	E_{pw} = 64 Ry	5.26	2.48	6.46
	E_{pw} = 70 Ry	5.26	2.48	6.50
	Pseudopotential (Mixed basis) [a]	5.29	2.41	6.77
	FLAPW [b]	5.225±0.005	2.4±0.4	6.56±0.03
	Experiment	5.41	1.68-1.73	4.28
Ni	Present work			
	E_{pw} = 64 Ry	6.56	2.31	6.99
	E_{pw} = 70 Ry	6.58	2.46	7.20
	E_{pw} = 75 Ry	6.58	2.25	7.24
	KKR [c]	6.55	2.27	5.70
	Experiment	6.66	1.84	4.44

[a]Reference 5.
[b]Reference 13.
[c]Reference 15.

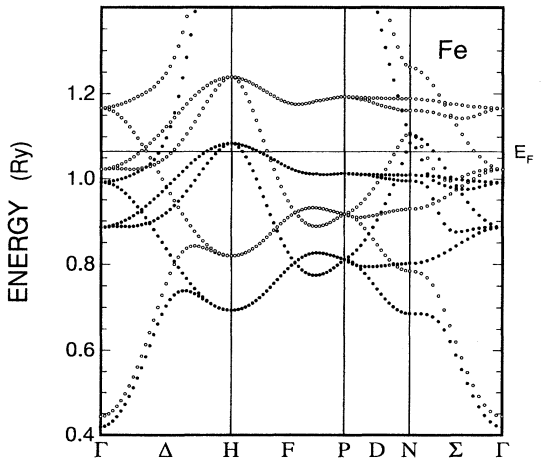

FIG. 4. Calculated band structure of bcc iron at lattice constant a=5.25 a.u. Closed circles are for majority-spin states and open circles are for minority-spin states. The Fermi level is indicated by a horizontal line.

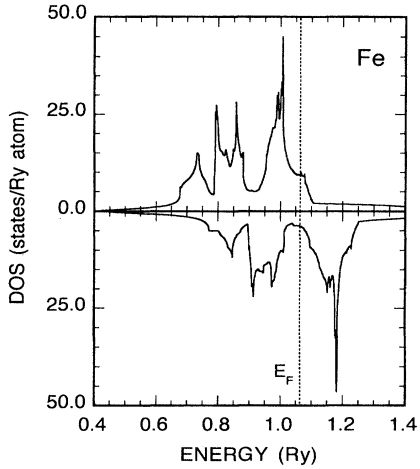

FIG. 6. Calculated density of states of bcc iron at lattice constant a=5.25 a.u. The Fermi level is indicated by a broken line. The upper (lower) panel is for the majority (minority) -spin states.

gies for the $3d$ orbitals, which characterize the magnetic properties. The intra-atomic Coulomb correlation energy is defined by $E[(3d)^{n+1}]+E[(3d)^{n-1}]-2E[(3d)^n]$, where $E[(3d)^n]$ is the total energy of an atom with n electrons in the $3d$ orbitals. The values calculated using the pseudopotentials are 1.134 Ry for the Fe^{2+} ion and 1.246 Ry for the Ni^{2+} ion. These values are within 3% of the all-electron values, which are 1.106 and 1.214 Ry, respectively.

The scattering properties of a pseudopotential provide another important test of its transferability. Figure 2 shows the logarithmic derivatives of the all-electron and pseudopotential $3d$ wave functions at the reference configuration and the ground-state configuration for iron at $r=2.2$ a.u. In the former case, no significant discrepancy from the all-electron results can be seen within 0.5 Ry of the reference eigenvalues. The same accuracy is obtained in the fully polarized state. These results indicate that the present pseudopotentials will be applicable to solid systems in a magnetic state. The actual application for solids will be discussed in the next section.

The exchange splitting, the energy difference between electrons in the same orbital but with different spin orientations, in principle may arise from either a modification of the shape of the wave functions or from a difference in the exchange-correlation potential seen by the majority and minority spins. According to our calculations, spin polarization does not affect the shape of the wave functions significantly. The exchange splitting primarily results from the difference between the exchange-correlation potentials.

In Fig. 3 we compare the exchange-correlation potential differences between majority and minority spins given by the pseudopotential and all-electron calculations. Because the exchange-correlation potential is a simple function of the electron density in LSDA, the potential difference is largest

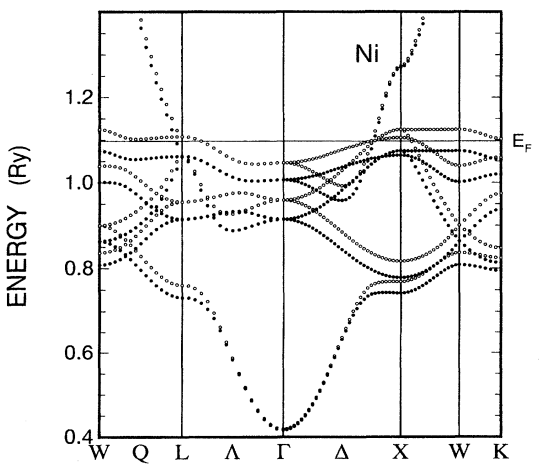

FIG. 5. Calculated band structure of fcc nickel at lattice constant a=6.55 a.u. The Fermi level is indicated by a horizontal line. Notations are the same as those in Fig. 4.

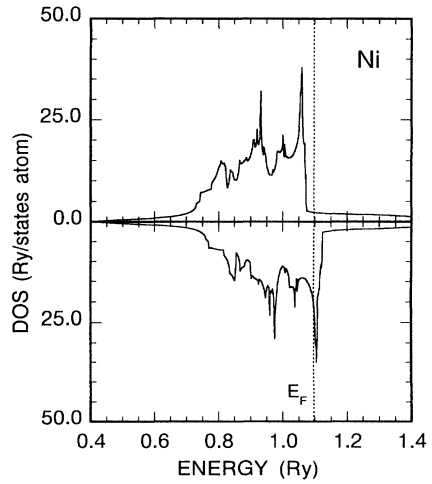

FIG. 7. Calculated density of states of fcc nickel at lattice constant a=6.55 a.u. The Fermi level is indicated by a broken line. The upper (lower) panel is for the majority (minority) -spin states.

near the peak of the $3d$ wave function in both calculations. The pseudopotential calculation yields an exchange-correlation potential difference which is similar to that of the all-electron calculation except for a shift in location due to the shift in the valence pseudo-wave-function peak. We believe that the accuracy in the magnetic properties of the present pseudopotential calculation derives from this similarity.

III. BCC IRON AND FCC NICKEL

The total energies of bcc iron and fcc nickel are calculated with a plane-wave basis set as a function of volume. The integration over occupied states are performed with 40 and 60 k points in the irreducible part of the bcc and fcc Brillouin zones, respectively. This k-point sampling gives total energy convergence to better than 1 mRy/atom. The partial-core-correction scheme[12] is used to speed up the computation of the exchange-correlation energy. The core charge density is replaced by a smooth function inside a radius of 0.6 a.u. This partial-core approximation introduces an error which is less than 1 mRy/atom in the spin-flip energy.

Table II shows the calculated structural parameters obtained by fitting the total energies to the Murnaghan's equation of state. The results indicate that cutoff energies of 64 and 70 Ry for iron and nickel, respectively, are large enough to obtain converged results for the structural properties. These results are also compared with the results of previous calculations. Previous all-electron results vary by 1% or more[13] depending on the details of the calculation methods used. The present results are within this range. The notable difference in the cohesive energy of nickel may be due to the muffin-tin approximation used in the KKR calculation. The disagreement with experimental values for the cohesive energies is now well established to be a limitation of the LSDA.[14]

Figures 4 and 5 show the band structures calculated for Fe and Ni using a plane-wave basis set with the cutoff energy of 64 Ry for both Fe and Ni. The convergence error of the eigenvalues is about 0.01 eV for Fe and less than 0.03 eV for Ni. The d-band widths of iron measured at the Γ point are 1.47 and 1.99 eV for the majority and minority spins, respectively. An extensive study of bcc Fe has been performed by Hathaway *et al.*[13] using the full-potential linearized APW (FLAPW) method. The discrepancy from their values of 1.50 and 1.99 eV (Ref. 16) is 0.03 eV or less. Further, our computed exchange splittings at the Γ point are 1.80 and 2.32 eV for the $\Gamma_{25'}$ and Γ_{12} states, respectively, as compared to the corresponding all-electron values of 1.83 and 2.32 eV.

The present calculation yields a d-band width for nickel measured at the Γ point of 1.26 eV (1.20 eV) for the majority (minority) spin state. The KKR method yields a d-band width of 1.08 eV (1.15 eV).[15] We calculate exchange splittings of 0.61 and 0.55 eV for $\Gamma_{25'}$ and Γ_{12}, respectively. These values differ 0.01 and 0.10 eV, respectively, from the KKR result. In comparison with the case of iron, the discrepancy from the KKR result is rather large as seen in the cohesive energies.

The calculated densities of states shown in Figs. 6 and 7 are obtained as follows. First, exact diagonalizations are performed on $8\times8\times8$ mesh points in the first Brillouin zone. The obtained eigenvalues are interpolated with the scheme by Koelling and Wood[17] on denser mesh points. Converged estimates for the Fermi energy and the magnetic moment were obtained by using a $20\times20\times20$ division with errors of less than 0.001 eV and 0.01 μ_B/atom, respectively. The densities of states in the figures are very similar to the results obtained with the FLAPW method[13] and the KKR method.[15] The magnetic moment at the equilibrium volume is calculated from the density of states to be 2.07 μ_B/atom for bcc iron, which should be compared with the all-electron value of 2.06 μ_B/atom.[13] Although some rather large discrepancies are seen in the case of the electronic structure of nickel, the agreement of the magnetic moments is excellent: Both methods yield the same value, 0.59 μ_B/atom.

IV. CONCLUSIONS

In this study, we have shown that optimized pseudopotentials can be applied to transition metals to obtain structural, electronic, and magnetic properties with high accuracy despite a large difference in the amplitudes of the wave functions in the core region. Replacing the wave functions by optimized pseudo wave functions does not significantly affect the magnetic properties, since the main effect is to shift both the wave function and the exchange-correlation potential in real space while preserving the magnetic moment value. The calculated cohesive, structural, and magnetic properties of bcc iron and fcc nickel reproduce the results of previous all-electron calculations.

ACKNOWLEDGMENTS

This work was supported by National Science Foundation Grant No. DMR-9120269 and by the Director, Office of Energy Research, Office of Basic Energy Sciences, Materials Sciences Division of the U.S., Department of Energy under Contract No. DE-AC03-76SF00098. Supercomputer time was provided by the National Science Foundation at the National Center for Supercomputing Applications in Illinois. A. M. R. acknowledges financial support from IBM.

*Permanent address: National Research Institute for Metals, Tsukuba 305, Japan.

†Permanent address: Department of Chemistry and Laboratory for Research into the Structure of Matter, University of Pennsylvania, Philadelphia, PA 19104.

[1] A. M. Rappe, K. M. Rabe, E. Kaxiras, and J. D. Joannopoulos, Phys, Rev. B **41**, 1227 (1990).

[2] N. Troullier and J. L. Martins, Phys. Rev. B **43**, 1993 (1991).

[3] D. Vanderbilt, Phys. Rev. B **41**, 7892 (1990).

[4] H. S. Greenside and M. A. Schlüter, Phys. Rev. B **27**, 3111 (1983); *ibid.* **28**, 535.

[5] J. Zhu, X. W. Wang, and S. G. Louie, Phys Rev. B **45**, 8887 (1992).

[6] O. Gunnarson and B. I. Lundqvist, Phys. Rev. B **13**, 4274 (1976).

[7] P. Hohenberg and W. Kohn, Phys. Rev. **136**, B864 (1964).

[8] C. S. Wang, B. M. Klein, and H. Krakauer, Phys. Rev. Lett. **54**, 1852 (1985).

[9] D. M. Ceperley and B. J. Alder, Phys. Rev. Lett. **45**, 566 (1980).

[10] J. Perdew and A. Zunger, Phys. Rev. B **23**, 5048 (1981).
[11] D. R. Hamann, M. Schlüter, and C. Chiang, Phys. Rev. Lett. **43**, 1494 (1979).
[12] S. G. Louie, S. Froyen, and M. L. Cohen, Phys. Rev. B **26**, 1738 (1982).
[13] K. B. Hathaway, H. J. F. Jansen, and A. J. Freeman, Phys. Rev. B **31**, 7603 (1985).
[14] S. Fahy, X. W. Wang, and S. G. Louie, Phys. Rev. B **42**, 3503 (1990).
[15] V. L. Moruzzi, J. F. Janak, and A. R. Williams, *Calculated Electronic Properties of Metals* (Pergamon, New York, 1978).
[16] Since the equilibrium lattice constant is slightly different from the lattice constant used by Hathaway *et al.* to obtain the band structure, we interpolated their energies at the present lattice constant.
[17] D. D. Koelling and J. H. Wood, J. Comput. Phys. **67**, 253 (1986).